"Double-tailed lipid modification as a promising candidate for oligonucleotide delivery in mammalian cells." Ugarte-Uribe, B., Grijalvo, S., Busto, J. V., Martín, C., Eritja, R., Goñi, F. M., Alkorta, I. Biochim. Biophys. Acta (General subjects), 1830, 4872-4884 (2013). doi: 10.1016/j.bbagen.2013.06.013

Double-tailed lipid modification as a promising candidate for oligonucleotide delivery in mammalian cells

Begoña Ugarte-Uribe [a,1], Santiago Grijalvo [b,2], Jon V. Busto [a,3], César Martín [a], Ramón Eritja [b,2], Félix M. Goñi [a], Itziar Alkorta [a,*]

[a] Department of Biochemistry and Molecular Biology, UPV/EHU and Biophysics Unit (CSIC, UPV/EHU), Barrio Sarriena s/n, 48940 Leioa, Spain.

[b] Networking Center on Bioengineering, Biomaterials and Nanomedicine (CIBER-BBN); Institute for Research in Biomedicine (IRB Barcelona) and Institute for Advanced Chemistry of Catalonia (IQAC-CSIC), Baldiri Reixac 10, E-08028 Barcelona, Spain.

* Corresponding author. Tel: +34-94-6012568; fax: +34-94-6013500. *Email address*: itzi.alkorta@ehu.es (I. Alkorta)

[1] Current Address: Membrane Biophysics, Max Planck Institute for Intelligent Systems, Stuttgart, Germany.

[2] Current Address: IQAC-CSIC, Jordi Girona 18-26, 08034 Barcelona, Spain.

[3] Current Address: Cellular Dynamics and Cell Patterning, Max Planck Institute of Biochemistry, Am Klopferspitz 18, 82152 Martinsried, Germany.

Abstract

Background: The potential use of nucleic acids as therapeutic drugs have triggered the quest for oligonucleotide conjugates with enhanced cellular permeability. To this end, the biophysical aspects of previously reported potential lipid oligodeoxynucleotide conjugates were studied including its membrane-binding properties and cellular uptake.

Methods: These conjugates were fully characterized by MALDI-TOF mass spectrometry and HPLC chromatography. Their ability to insert into lipid model membrane systems was evaluated by Langmuir balance and confocal microscopy followed by the study of the internalization of a lipid oligodeoxynucleotide conjugate bearing a double-tail lipid modification (C_{28}) into different cell lines by confocal microscopy and flow cytometry. This compound was also compared with other lipid containing conjugates and with the classical lipoplex formulation using Transfectin as transfection reagent.

Results: This double-tail lipid modification showed better incorporation into both lipid model membranes and cell systems. Indeed, this lipid conjugation was capable of inserting the oligodeoxynucleotide into both liquid-disordered and liquid-ordered domains of model lipid bilayer systems and produced an enhancement of oligodeoxynucleotide uptake in cells, even better than the effect caused by lipoplexes. In addition, in β_2 integrin (CR3) expressing cells this receptor was directly involved in the enhanced internalization of this compound.

Conclusions: All these features confirm that the dual lipid modification (C_{28}) is an excellent modification for enhancing nucleic acids delivery without altering their binding properties.

General significance: Compared to the commercial lipoplex approach, oligodeoxynucleotide conjugation with C_{28} dual lipid modification seems to be promising to improve oligonucleotide delivery in mammalian cells.

Keywords

Lipid oligonucleotide conjugates

Model membrane systems

Cellular uptake and localization

Abbreviations

LOC, lipid oligonucleotide conjugate; TLC, thin-layer chromatography; ACN, acetonitrile; TEAA, triethylammonium acetate; TOF, time-of-flight; ODN, oligodeoxynucleotide; CPG, controlled-pore glass; PBS, phosphate-buffered saline; DOPC, 1,2-*dioleyl*-*L*-*α*-phosphatidylcholine; GUV, giant unilamellar vesicle; SPB, supported planar bilayer; eSM, egg sphingomyelin; Chol, cholesterol; L_d, liquid-disordered; L_o, liquid-ordered; MLV, multilamellar vesicle; SUV, small unilamellar vesicle; AFM, atomic force microscopy; DMEM, Dulbecco's modified Eagle's medium; FBS, fetal bovine serum; GMFI, Geometric Mean Fluorescence Intensity; PFA, paraformaldehyde

1. Introduction

The ability of some small nucleic acid-based molecules such as DNA decoys, triple helix forming oligonucleotides, RNA decoys, antisense oligonucleotides, ribozymes, DNAzymes, siRNAs or aptamers to silence specific genes or to inhibit the biological activity of specific proteins has generated great interest for their use as research tools and therapeutic agents [1-3]. Unfortunately, biological applications of oligonucleotides meet a huge limitation namely cellular accessibility [4]. In fact, phospholipid bilayers represent a strong barrier for the highly negatively charged phosphodiester backbone of the oligonucleotides, leading to an extremely poor penetration across the cell membrane. Nevertheless, simple elimination of the anionic charge does not improve cellular uptake, as evidenced by chemically modified neutral backbone-containing oligonucleotides [5]. Therefore developing an appropriate delivery system in order to achieve their efficient cellular uptake remains an important challenge. In this regard, the use of lipid-based systems has long been considered as a possible method to solve cell permeation problems [6].

The introduction of both neutral and cationic lipids into oligonucleotides is one of the approaches to improve the delivery of these kinds of biomolecules, thereby favoring interaction with, or insertion into the plasma membrane along with improving their stability compared to unmodified oligonucleotides [7, 8]. To date several lipophilic molecules, including cholesterol, phospholipids, α-tocopherol and alkyl chains, have been conjugated to oligonucleotides in order to obtain better clinically acceptable therapeutic drugs [9-14]. The main goal of these lipophilic compounds is to improve oligonucleotide delivery and to enhance their cellular uptake via receptor-mediated endocytosis by increasing the membrane permeability without altering the potential properties of the nucleic acid molecule, thereby achieving the desired gene expression inhibition [6, 15-19].

Recently, our group reported the synthesis of several lipid oligonucleotide conjugates (LOCs) series containing neutral and cationic lipids at their 3'- and 5'-termini and their evaluation *in vitro* in RNA interference [20, 21]. We observed that all lipid modifications did not disrupt the RNAi machinery obtaining in some cases promising results in inhibiting gene expression without using a transfection agent. Indeed, the siRNA carrying the C_{28} moiety at the 5'-end of the passenger strand showed the best inhibitory effects in the absence of the transfecting agent Oligofectamine [21]. It is well-known that cellular uptake and the intracellular distribution of nucleic acids may depend on both their surface properties and

their interactions with the cell membrane. In the present work, we study such interactions induced by LOCs conjugates, specially C_{28} moiety containing LOC (Fig. 1), using three model membrane systems (*i.e.*, monolayers, giant unilamellar vesicles and supported planar bilayers), and several cell lines. As shown in Fig. 1, the majority of the lipid modifications at both 3'- and 5'-termini were neutral (Fig. 1, compounds **4-7**) based on SNALP formulations; except for one of them in which the lipid attached into the oligonucleotide at 3'-termini showed a polar group at the end of the lipophilic tail (Fig. 1, compound **3**), mimicking the effect produced by lipoplex complexes.

2. Materials and methods

2.1. General methods and materials

All reactions were carried out under argon positive pressure in anhydrous solvents. Commercially available reagents and anhydrous solvents were used without further purification. Solvents were distilled prior to use and dried using standard methods. Analytical samples were homogeneous as confirmed by thin-layer chromatography (TLC) and yielded spectroscopic results were consistent with the assigned structures. TLC was performed on silica gel (Alugram Sil G/UV).

2.2. HPLC conditions

Conditions for semipreparative HPLC: HPLC solutions were Solvent A [5% acetonitrile (ACN) in 100 mM triethylammonium acetate (TEAA), pH 6.5] and Solvent B (70% ACN in 100 mM TEAA, pH 6.5). Column: PRP-1 (Hamilton) 250 x 10 mm. Flow rate 3 ml/min linear gradient from 15 to 100% in B (DMT*on*) and 0 to 85% in B (DMT*off*) was used with UV detection at 260 nm. Conditions for analytical HPLC: HPLC solutions were Solvent A [5% ACN in 100 mM TEAA, pH 6.5] and Solvent B (70% ACN in 100 mM TEAA, pH 6.5). Column: XBridge OST C18 2.5 µm. Flow rate 1 ml/min linear gradient from 0 to 85% in B (DMT*off*) were used with UV detection at 260 nm. Mass spectra were recorded on a MALDI Voyager DE RP time-of-flight (TOF) spectrometer (Applied Biosystems, Framingham). Two different matrix were used: 2,4,6-trihydroxiacetophenone (10 mg/ml in ACN:H_2O 1:1 v/v); ammonium citrate (50 mg/ml in H_2O).

2.3. Synthesis of modified oligonucleotide conjugates with lipids at either 5'- or 3'-termini

Oligodeoxynucleotides (ODNs) carrying lipids at the 3′-termini were prepared in a DNA synthesizer (Applied Biosystems 3400) using standard 2-cyanoethyl phosphoramidites and modified controlled-pore glass (CPG) solid supports (Suppl. Scheme S1, compounds **CPG-1**, **CPG-2** and **CPG-3**). These supports were prepared according literature [20, 21].

ODNs carrying lipids at the 5′-termini were prepared using the same standard 2-cyanoethyl phosphoramidites and the appropriate lipid phosphoramidites (Suppl. Schemes S1 and S2, compounds **I** and **II**). The syntheses were carried out on CPG supports carrying the 2-(*N*-[9*H*-fluoren-9-yl-

methoxycarbonyl]-4-aminobutyl)propane-1,3-diol linker (Glen Research) to yield oligonucleotide conjugates carrying an aliphatic amino group at the 3′-end and the lipid moiety at 5'-termini. In both cases, after ammonia deprotection (overnight, 55℃) , the resulting modified oligodeoxynucleotides at both 3'- (Fig. 1 and Table 1, compounds **3-5**) and 5'-termini (Fig. 1 and Table 1, compounds **6-7**) were purified by HPLC (see conditions below) and conjugates were characterized by mass spectrometry (Table 1). Sequence **6** was obtained by using commercially available 3'-amino modifier CPG resin and standard 2-cyanethyl phosphoramidites purifying it according to conditions described below.

ODNs carrying lipids at the 3′-termini and an amine group at 5'-termini were prepared using standard 2-cyanethyl phosphoramidites and modified CPG solid supports (Suppl. Scheme S1, compounds **CPG-2** and **CPG-3**) as described above. The introduction of the amino group at the 5'-end was achieved using the commercially available 5'-amino-modifier-C6-Tfa phosphoramidite (Glen Research) obtaining the corresponding LOC conjugates (Table 1, compounds **8** and **9**). The amine oligonucleotide conjugates were used without further purification in the next step.

Compounds **1**-**9** (Table 1) were characterized by MALDI-TOF mass spectrometry and HPLC chromatography (Suppl. Figs. S1-S7 and S15-S16).

2.4. Synthesis of modified oligonucleotide conjugates with lipids at either 3'- or 5'-termini carrying Alexa 488 as a fluorescent dye

A solution of the deprotected amine oligonucleotide conjugates described above were passed through a column filled with *Dowex* 50x2, sodium form to remove the interfering ammonium ions coming from the cleavage step. Conjugates **6**, **7**, **8** and **9** (Table 1) were dissolved with 50 µL of an aqueous solution of 0.2 M $NaHCO_3$ (pH 9). Then, 1.1 equiv of Alexa Fluor 488 tetrafluorophenyl ester dissolved in 30 µL DMF was added to the solution and left to react overnight at room temperature. The mixture was concentrated to dryness, and the residue was dissolved in H_2O (1 ml). The green solutions were purified with *Sephadex* G-25 (NAP-10 Column), and the corresponding oligonucleotide fractions were analyzed and purified by semi-preparative HPLC. In the preparation of sequences **12** and **13** (Fig. 1 and Table 1) we were not able to separate by HPLC the labeled and unlabelled conjugates (Suppl. Figs. S10 and S11). For this reason the mixtures were used in the study.

Compounds **10**-**14** (Table 1) were characterized by MALDI-TOF mass spectrometry and HPLC chromatography (Suppl. Figs. S8-S11).

2.5. Synthesis of lipid oligonucleotide conjugates carrying Cy5 fluorescent dye at the 5'-end

In order to obtain the corresponding oligonucleotide conjugates with Cy5 fluorescent label attached at 5'-termini, we used the same modified CPG solid supports (Suppl. Scheme S1, compounds **CPG-1**, **CPG-2** and **CPG-3**). The last coupling was carried out manually, introducing the commercially available Cy5 phosphoramidite (Glen Research) into the corresponding CPG resins. DNA syntheses were carried out using the dmf-dG-CE phosphoramidite (Link Technologies). After deprotection with ammonia solution (6 h

at room temperature) and purification by semi-preparative HPLC (see below), the corresponding lipid oligonucleotide conjugates with Cy5 were obtained.

Compounds **15**-**18** (Table 1) were characterized by MALDI-TOF mass spectrometry and HPLC chromatography (Suppl. Figs. S12-S14 and S17).

All conjugates were lyophilized and dissolved in phosphate-buffered saline (1× PBS) for further experiments with lipid membrane model and cell systems.

2.6. Surface tension measurements

The studies were carried out at 22ºC using a µThrough-S equipment (Kibron Inc., Finland) consisting of 2-cm rounded multi-well plate that allowed for 1 ml subphase measurements. For possible LOC monolayer formation, each LOC was injected into the subphase through an adjusted hole without previous lipid spreading, following LOC transition to the interface in terms of changes in surface pressure. For possible LOC interaction with lipids, 1,2-*dioleyl*-*L*-*α*-phosphatidylcholine (DOPC) monolayers were formed by spreading a small amount of lipid (about 2 nmol) in chloroform:methanol (2:1, v/v) solution over 1× PBS solution. After allowing for solvent evaporation, each LOC was added into the subphase and the changes in surface pressure were recorded.

2.7. Giant unilamellar vesicle (GUV) preparation

Sucrose-enclosing GUVs were prepared using the electroformation method as described previously [22]. DOPC/egg sphingomyelin (eSM)/cholesterol (Chol) (2:2:1) stock solutions were prepared to contain 0.4 mol% DiO (3,3′-dioctadecyloxacarbocyanine) or DiD (1,1′-dioctadecyl-3,3,3′,3′-tetramethylindodicarbocyanine) (Invitrogen). Both fluorescent probes partition within liquid-disordered phases in liquid-disordered-liquid-ordered (L_d-L_o) phase-coexistence-showing bilayers. Vesicles were generated in a 300 mM sucrose solution at 60ºC, a temperature rendering bilayers in a fluid phase state. 30 minutes after electroformation and vesicle equilibration at room temperature, 50 µl vesicles were pipetted onto 250 µl of an equiosmolar 1× PBS buffer solution in Lab-Tek Chamber slides (Thermo Fisher Scientific, NY, USA).

2.8. Supported planar bilayer (SPB) preparation

Planar bilayer preparation on mica substrate was performed using the vesicle adsorption technique [23]. Briefly, DOPC/eSM/Chol (2:2:1) multilamellar vesicles (MLVs) were initially prepared by mixing the appropriate amount of synthetic pure lipids dissolved in chloroform/methanol (2:1, v/v). As in GUVs preparation, 0.4% of the lipophilic fluorescent probes DiO or DiD in chloroform/methanol (2:1) were also pipetted into the lipid mixture in order to visualize the L_d phase of these bilayer systems. Small unilamellar vesicles (SUVs) were then obtained after sonication of the MLV suspension at 60℃ for 1 h in a FB-1504 9 bath sonicator (Fisher Scientific, Waltham, MA). 60 µl SUVs was added to a 1.2-cm^2 freshly cleaved mica substrate previously mounted onto a BioCell coverslip-based liquid cell for atomic force microscopy (AFM)

measurements (JPK Instruments, Berlin, Germany) and hydrated with 120 µl 1× PBS, containing 10 mM $CaCl_2$ at 60℃. Final lipid concentration was 150 µM. Vesicles were left to adsorb for 30 min at 55℃. Non-adsorbed vesicles were then discarded by washing the samples 10 times with assay buffer at 60℃ in the absence of $CaCl_2$. Finally, 400 µl PBS was added to the SPBs at 60℃ and left to equilibrate at room temperature for 45 min before confocal microscopy image acquisition.

2.9. Experiments of LOC incorporation into GUVs and SPBs by confocal microscopy

Images were obtained in an inverted fluorescence confocal microscope (Leica TCSSP5, Leica Microsystems, Wetzlar, Germany). Briefly, 8 well-Lab-Tek Chamber slides pre-treated with bovine serum albumin (to avoid vesicle rupture) where GUVs were sedimented at the bottom of each well containing 1× PBS due to the higher density of the enclosed sucrose, or biocell-liquid-cell containing SPBs were placed on top of the microscope followed by image acquisition with a 40× LD objective using an excitation wavelength of 488 and 633 nm for DiO and DiD, respectively, and the emission was retrieved between 505-540 nm for DiO and 655-795 nm for DiD. Binding of Alexa 488-labelled and Cy5-labelled LOCs to fluorescently labelled GUVs or SPBs was observed under the microscope in sequential mode imaging, using the same excitation and emission wavelengths for Alexa 488 and Cy5 as for DiO and DiD, respectively. Image treatment was performed using Leica Application Suite software.

2.10. Cell Lines

HeLa (cervical carcinoma) cell line was kindly provided by Prof. Alfredo Berzal (Instituto de Parasitología y Biomedicina "López-Neyra", CSIC, Granada, Spain). PANC-1, C2C12 and RAW 264.7 cell lines were generously donated by Prof. Antonio Gómez-Muñoz (Departamento de Bioquímica y Biología Molecular, EHU/UPV, Leioa, Spain). CHO K1, CHO CR3+, J774A.1 and J774A.1 CR3- cell lines were kindly provided by Prof. Cesar Martín (Unidad de Biofísica, Centro Mixto CSIC-UPV/EHU and Departamento de Bioquímica y Biología Molecular, EHU/UPV, Leioa, Spain).

HeLa cell line is the most commonly used human cell line in scientific research. In this study **U87.CD4.CXCR4** a human glioblastoma-astrocytoma cell line which expresses CD4 receptor and CXCR4 co-receptor in the cell surface was used. It has epithelial morphology and it is usually used as an *in vitro* model of human glioblastoma cells to investigate the cytotoxic effect of chemotherapeutic drugs towards cancer cells. **PANC-1** cell line is a human pancreatic carcinoma, epithelial-like cell line that is commonly used as an *in vitro* model of non-endocrine pancreatic cancer for tumorigenicity studies. **C2C12** cell line is a subclone of mouse myoblast that differentiates rapidly, forming contractile myotubes and producing characteristic muscle proteins. **RAW 264.7** cell line is a monocyte/macrophage cell line obtained from Abelson murine leukemia virus-induced tumour of BALB/c mice. This cell line was chosen due to the stable expression of β_2 integrin, CD11b/CD18 (CR3), on its cell surface. **CHO K1** and **CHO CR3+** cell lines are epithelial-like cell lines. In this study CHO CR3+ cell line was used because expresses β_2

integrin, CD11b/CD18 (CR3), in the cell surface. **J774A.1** and **J774A.1 CR3-** cell lines are monocyte/macrophage cell lines obtained from a BALB/c mice with reticulum-like sarcoma. As RAW 264.7, J774A.1 cell line also presentes a stable expression of β_2 integrin, CD11b/CD18 (CR3), on its cell surface. Additionally, J774A.1 CR3- cell line, which does not express β_2 integrin, was also used in this study.

2.11. Cell Culture

Cells were cultured as exponentially growing subconfluent monolayers and maintained in Dulbecco's modified Eagle's medium (DMEM, PAA Laboratories GMBH) supplemented with 10% fetal bovine serum (FBS) (Invitrogen), 4 mM L-Glutamine (Sigma-Aldrich), Mycokill AB (PAA Laboratories GMBH), and penicillin/streptomycin (100 units/ml and 100 µg/ml, respectively) (Invitrogen) in a humidified atmosphere consisting of 5% CO_2 and 95% air. The culture media used for U87.CD4.CXCR4, CHO CR3+ and J774A.1 CR3- cells were also supplemented with 1 µg/ml puromycin and 300 µg/ml Geneticin (G418 sulphate), 150 µg/ml hygromycin B and 500 µg/ml G418, and 1.5 µg/ml puromycin, respectively.

2.12. Mycoplasma detection assay

Venor®GeM Mycoplasma Detection Kit was used to discard cell cultures contaminated with *Mycoplasma*.

2.13. Cell cytotoxicity assay

Cells were seeded in 96-well plates (2.5×10^3 cells/well) and allowed to attach overnight in appropriate growth medium. The medium was then replaced with 100 µl OptiMEM serum-free medium (Gibco, Invitrogen) in the absence or presence of oligonucleotide conjugates and cells were incubated for 24 h or 48 h at 37ºC. Cell growth was estimated by measuring the rate of reduction of the tetrazolium dye MTS to formazan, as previously described [24, 25]. The absorbance of the medium without cells was subtracted from all absorbance values and the control values were considered as 100% of cell viability. Relative cell viability of individual samples was calculated by normalizing their absorbance to that of the corresponding control sample.

2.14. Cellular binding/uptake studies by flow cytometry

Cy5- or Alexa 488-labelled ODN was mixed with Transfectin cationic lipid reagent (BIO-RAD), forming ODN-lipoplexes in order to compare conjugation and complexation patterns. Lipoplex formation and incubation parameters (4 h at 37ºC) were set depending on the maximum transfection yield described for Transfectin complexes, following manufacturer's instructions. Cells were seeded at 1.25×10^5 cells/well in 24-well plates and incubated overnight in appropriate growth medium. Then cells were incubated in the presence of Cy5- or Alexa 488-labelled LOCs, ODN and ODN-lipoplexes at 37℃ for 4 h. All these

experiments were performed using OptiMEM because the transfection efficiency of several standard transfection reagents is reduced in the presence of serum [26-30]. After incubation, cells were completely dissociated in 0.5% Trypsin-EDTA (Invitrogen). Trypsin treated cells were washed by centrifugation at 520 $\times$ *g* for 10 min and then resuspended into ice-cold 1$\times$ PBS, followed by a flow cytometry analysis (FACSCalibur, Beckton Dickinson) analyzing 10,000 cells per sample. The fluorescence of Alexa 488-labelled oligonucleotides remaining at the cellular surface was also quenched with 0.2% Trypan Blue (final concentration) (Sigma-Aldrich), and subsequently, the fluorescence corresponding to the internalized oligonucleotides was measured. Alexa 488 fluorescence was measured using an air-cooled 488 nm argon-ion laser, collecting emission signals by FL1 detector. In the case of Cy5, an air-cooled 633 helium-neon ion laser was used and Cy5 emission was collected by FL4 detector. GMFI (Geometric Mean Fluorescence Intensity) data of histograms were used for analysis using WinMDI 2.9 and Cell Quest (BD Biosciences) softwares. For determining the role of CR3 receptor in LOC uptake, these assays were also performed in the presence of fibrinogen, a natural ligand of β_2 integrin.

2.15. Cellular localization assays by confocal microscopy

Cy5- or Alexa 488-labelled ODN was also mixed with Transfectin, forming ODN-lipoplexes. Cells were seeded in 8 well-Lab-Tek Chamber slides (5×10^4 cells/well) pre-treated with Poly-L-lysine solution or in 96 well-BD Falcon™ Tissue Culture Treated Imaging plates (BD Biosciences) (2×10^4 cells/well) in and cultured overnight in appropriate growth medium. Cells were then incubated with Cy5- or Alexa 488-labelled LOCs for 30 min or 4 h at 37ºC in OptiMEM. After incubation, cells were washed three times, fixed with 4% (w/v) paraformaldehyde (PFA) for 15 min at room temperature, followed by nucleus staining with nuclear marker Hoechst 33258 (Molecular Probes, Invitrogen) for 10 min at room temperature. Finally, samples were visualized using Olympus IX 81 inverted fluorescence confocal microscope and image acquisition achieved with a digital camera (Axiocam NRc5, Zeiss). The slides were placed on top of the microscope for image acquisition with a 20$\times$ objective and zoom factor of 2$\times$, using excitation wavelengths of 405, 488 and 633 nm for Hoechst 33258, Alexa 488 and Cy5, respectively. The emission was recovered between 430-460 nm for Hoechst 33258, 505-525 nm for Alexa 488 and 660-IF nm for Cy5. Image treatment was performed using Fluoview v.50 software.

2.16. Cell-surface CR3 receptor staining assay by flow cytometry

Cell-surface CR3 expression was determined by using anti-CD11b FITC conjugated antibody (eBioscience) in CHO K1, CHO CR3+, J774A.1 CR3-, J774A.1 and RAW 264.7 cells. Cells were seeded at 1.25×10^5 cells/well in 24-well plates and incubated overnight in appropriate growth medium. Then cells were washed twice with 0.1% (w/v) BSA dissolved in 1X PBS, scrapped, centrifuged at 520 $\times$ *g* for 8 min at 4ºC and resuspended in 200 µl blocking solution [1X PBS containing 0.1% (w/v) BSA and 10% (v/v) FBS] for 15 min on ice to block unspecific binding of the antibody. After blocking reaction, cells were washed twice with 0.1% (w/v) BSA dissolved in 1X PBS and cell pellets were resuspended with 100 µl

anti-CD11b FITC conjugated antibody solution [1X PBS containing 0.1% (w/v) BSA and antibody (1:1000 dilution)]. Samples were incubated for 1 h on ice. Then, cells were washed twice with 0.1% (w/v) BSA dissolved in 1X PBS and fixed with 200 µl 4% (w/v) PFA for 20 min on ice. After fixing treatment, cells were washed twice with 0.1% (w/v) BSA dissolved in 1X PBS, followed by flow cytometric analysis. FITC fluorescence was measured using an air-cooled 488 nm argon-ion laser, collecting emission signals by FL1 detector.

2.17. Statistical analysis

All measurements were performed at least 3 times, and results are presented as mean ± s.d. Levels of significance were determined by a two-tailed Student's *t*-test, and a confidence level of greater than 95% ($p<0.05$) was used to establish statistical significance.

3. Results and discussion

3.1. Synthesis of LOCs

LOCs are a class of bioconjugates that are currently having a great attention from a therapeutic point of view, in particular in antisense and RNA interference therapies due to their unique physicochemical and biological properties. The introduction of lipid units into oligonucleotides at both 3'- and 5'-termini was performed as previously described [20, 21]. For the introduction of lipid units at the 3'-end we selected three lipid moieties of different length (12, 14 and 18 C atoms). The lipid-$C_{12}NH_2$ contained a terminal amine group. The lipid-C_{14} was a linear chain totally saturated and the lipid-C_{18} was a derivative of the linoleic acid with 2 unsaturations. As a model DNA sequence we selected the GEM91 sequence (5'-CTCTCGCACCCATCTCTCTCCTTCT-3'). This oligonucleotide carrying phosphorothioate linkages has anti-HIV-1 activity [31]. Modified CPG solid supports (Suppl. Scheme S1, compounds **CPG-1**, **CPG-2** and **CPG-3**) were used for the preparation of the corresponding conjugates (Table 1, compounds **3, 4** and **5**) modified at 3'-termini.

We selected two lipids for the 5'-position: A lipid carrying a saturated linear chain of 14 C atoms (lipid-C_{14}) and a lipid that contains two saturated lineal chains of 14 carbon atoms (lipid-C_{28}). In addition we introduced an amino group at the 3'-end for labeling purposes using standard commercial solid supports. The introduction of the lipid units was performed using the appropriate lipid phosphoramidites (Suppl. Schemes S1 and S2, compounds **I** and **II**) according the literature [32]. The corresponding conjugates **6** and **7** were obtained in good yields (Fig. 1). For comparative purposes the unmodified oligonucleotide sequence carrying the amine modifier at 3'-termini was prepared. All LOC conjugates were successfully characterized by HPLC and MALDI-TOF spectrometry (Table 1). The calculated masses were in good agreement with the measured values (Table 1).

3.2. Synthesis of fluorescence LOCs modified with Alexa Fluor 488 or Cy5 dyes

In order to carry out the membrane binding studies and the cellular uptake experiments, two different dyes were introduced into the ODN sequences at either 3' or 5'-termini. Alexa Fluor 488 (Life Technologies) was introduced into the LOC conjugates (Table 1, compounds **6** and **7**) along with the control oligonucleotide **2** (Table 1), taking advantage of the free amine moiety located at 3'-termini, through the post-synthetic approach and according to the literature [33]. The fluorescence oligonucleotide conjugates (compounds **10** and **11**) were obtained (Fig. 1) and confirmed by MALDI-TOFF mass spectrometry (Table 1). The same protocols were applied for the incorporation of Alexa Fluor 488 at 5'-termini to the rest of modified LOC conjugates (compounds **4** and **5**) and unmodified control sequences. But, in the case of the lipid conjugates (compounds **12** and **13**) it was not possible to separate the labelled and unlabelled compounds since according to HPLC analysis, mixtures of starting material and labelled oligonucleotides showed in both cases the same retention time.

Therefore, in order to achieve the fluorescence LOC conjugates modified with lipids at 3'-termini, we decided to incorporate Cy5 dye (Glen Research) into the previously synthesized conjugates (compounds **3-5**), through phosphoramidite chemistry approach. After deprotecting and purifying the oligonucleotide conjugates by semi-preparative HPLC, we could obtain the corresponding LOC conjugates labelled with Cy5 (compounds **15-17**) at their 5'-termini. Furthermore, we also obtained the unmodified Cy5-labelled oligonucleotide (compound **18**) which was used as a control. All conjugates were confirmed by MALDI-TOFF mass spectrometry (Table 1 and Suppl. Figs. S1-S17).

3.3. Surface activity of LOCs at air-water and lipid-water interfaces

The Langmuir lipid monolayer technique to mimic half a bilayer may be advantageous because properties such as composition, lateral pressure, surface elasticity and surface density are easily controlled [34, 35]. First, the surface-active properties of LOCs at an air-water interface were analyzed. All LOCs under study caused a dose-dependent increase in surface pressure at the air-water interface, except the LOC bearing $C_{12}NH_2$ at the 3' termini (compound **1**), which did not cause any change in surface pressure (data not shown). ODN itself was not surface-active either. After a certain time, which decreased with increasing LOC concentrations, surface pressure (π) remained constant (Fig. 2A). This constant value was operationally defined as an equilibrium value in this context. In order to compare the behaviour of LOCs under the same experimental conditions, π at 4,000 s was chosen as the equilibrium value. As observed in Fig. 2A, the final π (π_F) vs. LOC concentration curves reached a plateau at specific LOC concentration, which was used to test LOC insertion into DOPC monolayers at varying initial π values (Fig. 2B). All these data indicate that LOCs surface activity at air-water and lipid-water interfaces increased in the following order: ODN-3'-$C_{12}NH_2$ (compound **3**) < C_{14}-5'-ODN-3'-NH_2 (compound **6**) / ODN-3'-C_{14} (compound **4**) < NH_2-5'-ODN-3'-C_{18} (compound **9**) < C_{28}-5'-ODN-3'-NH_2 (compound **7**). Most importantly, only C_{28}-5'-ODN-3'-NH_2 (compound **7**) could be inserted into DOPC monolayers at initial lateral pressures above those assumed for cell membranes (around 30 mN/m), implying that this compound should be easily incorporated into the external leaflet of the cell membrane [36, 37].

3.4. Binding of LOCs to lipid bilayer systems

We investigated the spontaneous incorporation of LOCs into membranes bearing a curvature stress and surface charge comparable to those of the plasma membrane surrounding eukaryotic cells by using GUVs and SPBs [38-40]. These lipid bilayer systems were composed of DiO- or DiD-labelled DOPC/eSM/Chol (2:2:1) in order to analyze the effect of L_d and L_o lipid phase coexistence on LOC partitioning. All LOCs showed an apparently similar behaviour in both GUV and SPB systems (Suppl. Table S1).

Cy5-labelled ODN-$C_{12}NH_2$ (compound **15**) showed very weak fluorescence in the L_d phase of the GUVs that disappeared with prolonged light excitation (Suppl. Fig. S18). Moreover, Cy5-labelled ODN-$C_{12}NH_2$ (compound **15**) did not show any binding to SPB under these conditions (Suppl. Fig. S18). Large LOC aggregates were visualized in both GUV and SPB experiments. The reactive primary amine at the end of the alkyl chain could be protonated under these experimental conditions (pH 7.4) and bind the negatively charged backbone of the oligonucleotide via electrostatic interactions, leading to LOC aggregates [41, 42]. Indeed in the complexation strategy the formation of ODN-complexes/aggregates is based on the electrostatic interactions between reactive amines of the cationic agents and the negatively charged phosphate backbone of the oligonucleotides [43-45].

ODN-3'-C_{14} and ODN-3'-C_{18} compounds behaved differently when conjugated to Cy5 or Alexa 488 fluorophores. Cy5-labelled C_{14} and C_{18} containing LOCs (compounds **16** and **17**, respectively) were clearly seen in the L_d phase of GUVs and SPBs co-localizing with DiO dye (Suppl. Fig. S19), but when conjugated to Alexa 488 they did not show any remarkable interaction or insertion into the lipid bilayer, nor did Alexa 488-labelled C_{14}-5'-ODN (compound **10**) (Suppl. Fig. S20). This discrepancy may simply be due to the presence of the linker in combination with the size and hydrophobicity differences between the conjugated fluorophores, which could be incorporated with different efficiencies and/or interfere in the stability and/or properties of LOCs. Indeed, Cy5 is more hydrophobic than Alexa 488. Similarly other authors have reported that uptake of fluorescein-labelled ODN-conjugates could be altered due to the lipophilic nature of this fluorophore [5]. Moreover, since the labelling of these LOCs with Alexa 488 provided a mixture of labelled and unlabelled products that could not be separated by HPLC a 4% (w/v) agarose gel was performed in order to check the state of these LOCs. This assay revealed the poor stability of Alexa 488-labelled ODN-3'-C_{18} (compound **13**), which was prone to form aggregates, whereas Alexa 488-labelled ODN-3'-C_{14} (compound **12**) behaved similarly to the unlabelled or Cy5-labelled compounds (Suppl. Figs. S21 and S22).

Essentially, it could be reasonably expected that Alexa 488-labelled C_{28}-5'-ODN (compound **11**) would also spontaneously incorporate into L_o domains since it is long known that dual lipid modification appears to facilitate association with lipid rafts [46]. However, this LOC showed a remarkable and rapid incorporation into both lipid bilayer phases, being equally distributed between L_d and L_o domains after equilibration (Fig. 3). Similar observations have been reported by other authors who used a single

cholesterol moiety or two cholesteryl-TEG moieties containing double-stranded DNA structures, which did not exclusively partition into the L_o phase [47, 48]. This could be due to the fact that probes designed as cholesterol mimics usually do not satisfactorily reproduce the properties of pure cholesterol [47, 48]. Alternatively, the presence of two ether bonds in the structure of this LOC could be related to its homogeneous distribution in lipid membrane model systems, since ether-linked glycerophospholipids appear to be more loosely packed in membranes, thereby increasing their fluidity [49, 50]. In contrast, the fact that Alexa 488-labelled C_{28}-5'-ODN (compound **11**) compound, that possess two neighbouring alkyl chains, could be associated with model membranes is opposite to what it was observed by other authors who reported that a lipid-anchored oligonucleotide with two neighbouring alkyl chains may tend to form stable supramolecular structures in an aqueous environment, making it difficult to insert into preformed membranes [51]. In that case the oligonucleotide was conjugated to a chalcone moiety bearing longer alkyl chains ($2 \times C_{16}$) than those of C_{28}-5'-ODN ($2 \times C_{14}$). Our interpretation for this different behaviour relies on the higher hydrophobicity of the chalcone moiety with regard to the lipid anchor used in our work. Moreover, in SPB experiments reproducible, peculiar Alexa 488-enriched rounded structures were observed suggesting that these structures were at least in part formed by this LOC. Importantly, the homogeneous distribution of Alexa 488-labelled C_{28}-5'-ODN (compound **11**) in liquid domains co-existing in bilayers may provide several advantages in cell systems in terms of alternative internalization routes. Thus, once this LOC is inserted into the lipid bilayer, it could interact with a number of transmembrane proteins involved in distinct uptake pathways, thereby inducing its internalization through different routes.

3.5. Cell cytotoxicity, cellular binding, uptake and localization of LOCs in HeLa cells

The biological relevance of the above data was also studied by examining the uptake and subcellular localization of LOCs in HeLa cells, as this cell line is commonly used to study cell biology of uptake mechanisms [52-55]. *Mycoplasma* free HeLa cultures were used in order to avoid *Mycoplasma* infection-induced enhanced oligonucleotide uptake (Suppl. Fig. S23).

Cell cytotoxicity studies were performed to evaluate the possible toxic effects that these LOCs could trigger on HeLa cells. The data showed that these LOCs were neither cytotoxic nor antiproliferative at 5 µM, except for the LOC bearing a C_{28} moiety at the 5'-termini of the ODN, which decreased cell viability by over 30% and 60% during 24 and 48 h of incubation, respectively (Suppl. Fig. S24). This undesired result caused by this LOC is probably related to its high and rapid incorporation into membranes as well as to the presence of two ether bonds in this LOC, making it more difficult to degrade [56, 57].

The observations of binding/uptake experiments carried out with Cy5-labelled LOCs (Fig. 4A) were consistent with those observed in lipid model membrane systems, showing for LOCs bearing C_{14} and C_{18} moieties at the 3'-end of the ODN a remarkable binding/incorporation into both lipid model membranes and HeLa cell systems. Instead, Cy5-labelled ODN-3'-$C_{12}NH_2$ (compound **15**) showed only a slight increase in Cy5 fluorescence, similar to that obtained with Cy5-labelled control-ODN (compound **18**) (Fig. 4A). Similar results were observed by Love and co-workers, who reported that an optimized combination

of amine group and tail length is necessary to impart delivery activity since not all tested siRNA conjugates carrying a C_{12}-amine part moiety but differing in the amine presentation were successful for siRNA silencing, when formulated in combination with other lipids [58].

In addition to Cy5-labelled compounds, when HeLa cells were incubated with Alexa 488-labelled LOCs (Fig. 4B), they showed a higher cellular uptake as compared to Alexa 488-labelled control-ODN (compound **14**). In this regard, the following internalization behaviour was observed (from the lowest to the highest uptake profile): C_{14}-5'-ODN (compound **10**) / ODN-3'-C_{14} (compound **12**) < ODN-3'-C_{18} (compound **13**) < C_{28}-5'-ODN (compound **11**) (Fig. 4B). These results point to a better incorporation when longer and dual alkyl chains are conjugated with the ODN (*i.e.*, higher hydrophobicity). However, the latter observation is not fully in agreement with the results obtained in GUVs and SPBs with the Alexa 488-labelled LOCs bearing C_{14} or C_{18} moiety at the 3'- or 5'-termini since these LOCs did not show any noticeable incorporation into those membrane systems. Presumably, the experimental conditions chosen in uptake assays could not be ideal since under these conditions (4 h of incubation) precipitation may enhance the association of the LOCs with the cell surface, which could artifactually increase transfection rates of the LOCs that apparently do not insert into model membranes [59]. Similarly, these results are in agreement with the values obtained by Kubo and co-workers, who reported that palmitic acid (C_{16})-conjugated 21-nucleotide siRNA showed very weak fluorescence and insufficient RNAi effect in the absence of the transfecting agent Lipofectamine 2000 [60].

A further aspect that deserves some comment is that Alexa 488-labelled C_{28}-5'-ODN (compound **11**) showed higher internalization efficiency than that of Alexa 488-labelled ODN-lipoplexes (Fig. 4B). The latter result supports the observations reported by Grijalvo and co-workers, where the siRNA carrying the C_{28} moiety at the 5'-end of the passenger strand showed the best inhibitory effects in the absence of the transfecting agent Oligofectamine. Even more, this compound was the less active siRNA conjugate when combined with the transfecting agent [21]. Also, Lindner and co-workers convincingly demonstrated that myristoyl chains seem to play an important role in cationic liposome-mediated ODN delivery, as in a functional assay with ODN dimyristoyl analogs were the best cationic lipids for ODN transfection even in the absence of helper lipids [57].

Subcellular localization assays revealed that all LOCs, as well as control-ODNs, were visualized in the nucleus of HeLa cells, indicating that these lipid moieties conjugated to ODN do not interfere with the ODN destination (Fig. 5). Moreover, when the experiments were achieved either in the absence or presence of Transfectin same nuclear localization was observed, suggesting that conjugation and complexation approaches are equaly efficient (Fig. 5A and 5B).

Regarding cellular uptake and subcellular localization of LOCs, both Cy5- and Alexa 488-labelled LOCs were detected in the nucleus of HeLa cells as control ODNs (Fig. 5C and 5D).

In particular, the LOC containing a C_{28} moiety showed very high fluorescence localized in the nucleus of HeLa cells, with small intense fluorescent spots within it (Fig. 5D), suggesting that the concentration used (500 nM) in this assay could be saturating due to its high and rapid incorporation into cells.

Strikingly, when a lower concentration of this LOC was tested (50 nM), this compound was still capable of reaching the nucleus even after 30 min incubation, exhibiting a redistribution from the nucleus to the cytoplasmic membrane-bound compartments and membrane-like regions at longer periods of time (4 h) (Suppl. Fig. S25) [61]. The latter observation underscores the fact that the C_{28} lipid modification seems to be a promising moiety for small nucleic acid-based delivery since it does not interfere with the ODN destination or disrupt RNAi machinery when conjugated to siRNA [21].

3.6. Cell cytotoxicity, cellular binding, uptake and localization of C_{28}-5'-ODN in different cell lines

In order to demonstrate whether the results obtained by C_{28}-5'-ODN in HeLa cells were more generally applicable, eight more cell lines were examined (PANC-1, C2C12, CHO K1, CHO CR3+, J774A.1 CR3-, J774A.1, RAW 267). This LOC did not show any cytotoxic effect in all cell lines tested during 24 h of incubation (Fig. 6A). Subsequently, cellular uptake in these cell lines was analyzed. As expected, this LOC was better internalized in all cell lines tested compared to control-ODN (Fig. 6B). In particular, cells expressing CR3 receptor (*i.e.*, CHO CR3+, J774A.1 and RAW 264.7 cells) showed an enhanced LOC uptake even at 100 nM LOC, compared to cells lacking this receptor (*i.e.*, CHO K1 and J774A.1 CR3- cells). Indeed, J774A.1 and RAW 264.7 cells cell lines showed the highest uptake behaviour, in agreement with previous reports that suggested an enhanced ODN internalization mediated by β_2 integrins [62].

Despite the universality in membrane traffic, each cell type shows major unique features which obviously may influence intracellular delivery and traffic of the compound to be internalized [63]. Thus, it can be assumed that a particular cell type may select a specific uptake pathway for the internalization of a delivery system leading to an uptake efficiency, which may largely differ from those achieved by other cell types selecting different internalization routes. Related to this assumption, different results have been obtained in the cellular uptake (Fig. 6B) and subcellular localization (Fig. 7) where C_{28}-5'-ODN can be localized mostly in the nucleus of several but not all the cell lines tested under these experimental conditions. HeLa, PANC-1 and C2C12 cells first showed a nuclear LOC localization (30 min) that was further redistributed into the cell cytoplasm after longer time periods (4 h). Likewise, the transport of ODNs first to and then out of the nucleus has already been reported [61]. These observations are also in agreement with the results achieved by other authors who reported that the efficiency of cellular accumulation of lipophilic siRNAs was dependent upon the type of cell line tested [29].

By contrast, weak fluorescence was observed in the nucleus of U87.CD4.CXCR4, CHO CR3+, J774A.1 and RAW264.7 cell lines, being more noticeable at the cell cytoplasm both at short and long time periods. Finally, CHO K1 and J774A.1 CR3- cell lines showed very weak fluorescence at either 30 min or 4 h incubation times, suggesting an inefficient LOC uptake (Fig. 7).

3.7. Role of CR3 receptor in the enhancement of C_{28}-5'-ODN internalization

Related to the results obtained by CR3-presenting cell lines, previous investigations established an important role of these integrins in the enhancement of ODN internalization, thereby promoting a receptor-mediated endocytosis [62]. Thus, we examined whether this enhanced LOC internalization was mediated by this receptor. First cell surface CR3 expression was analyzed by flow cytometry. It was confirmed that CHO CR3+, J774A.1 and RAW 264.7 expressed CR3 integrin (Suppl. Fig S26). In this experiment CHO K1 and J774A.1 CR3- cell lines were used as negative controls.

To perform a deeper analysis of the involvement of CR3 integrin in the LOC uptake, soluble fibrinogen, a natural ligand for this integrin, was selected to compete with the LOC for the binding sites of this receptor, thereby blocking LOC internalization, as previously reported by other authors [62, 64-66]. In this experiment, again CHO K1 and J774A.1 CR3- cell lines were used as negative controls for CR3-mediated LOC internalization, assuming that in these cell lines LOC uptake did not vary in the presence of soluble fibrinogen as observed in Fig. 8A. On the contrary, in the presence of soluble fibrinogen the cellular uptake of this LOC was significantly blocked in CR3 presenting cells (*i.e.*, CHO CR3+, J774A.1 and RAW 264.7 cells). In fact, cellular uptake is inhibited at least up to 30% in the presence of 500 nM soluble fibrinogen. These results suggest the direct involvement of this receptor in LOC internalization (Fig. 8).

In conclusion, LOCs presenting longer or double-tailed lipid modifications (*i.e.*, with higher hydrophobicity) showed the best incorporation behaviour into both membrane lipid model and cell systems. Interestingly, the dual saturated lipid neighbouring moiety (C_{28}) at the 5'-termini of the ODN, which showed potencial silencing activity when conjugated to siRNA in the absence of tranfection reagents, turn out to be the most powerful lipophilic anchor tested, even better than the internalization provided by the commercial lipoplexes tested in this study, being capable of inserting into both L_d and L_o domains. Moreover, C_{28} lipid moiety provides better cellular incorporation of ODN without causing cytotoxicity in cells or altering the binding properties of the ODN itself, thereby enabling binding to different molecules, such as receptors present on the cell-surface, intracellular proteins involved in the intracellular ODN transport and target mRNA molecules. All these features make C_{28} lipid modification a good conjugation candidate for improving oligonucleotide delivery.

Figure captions

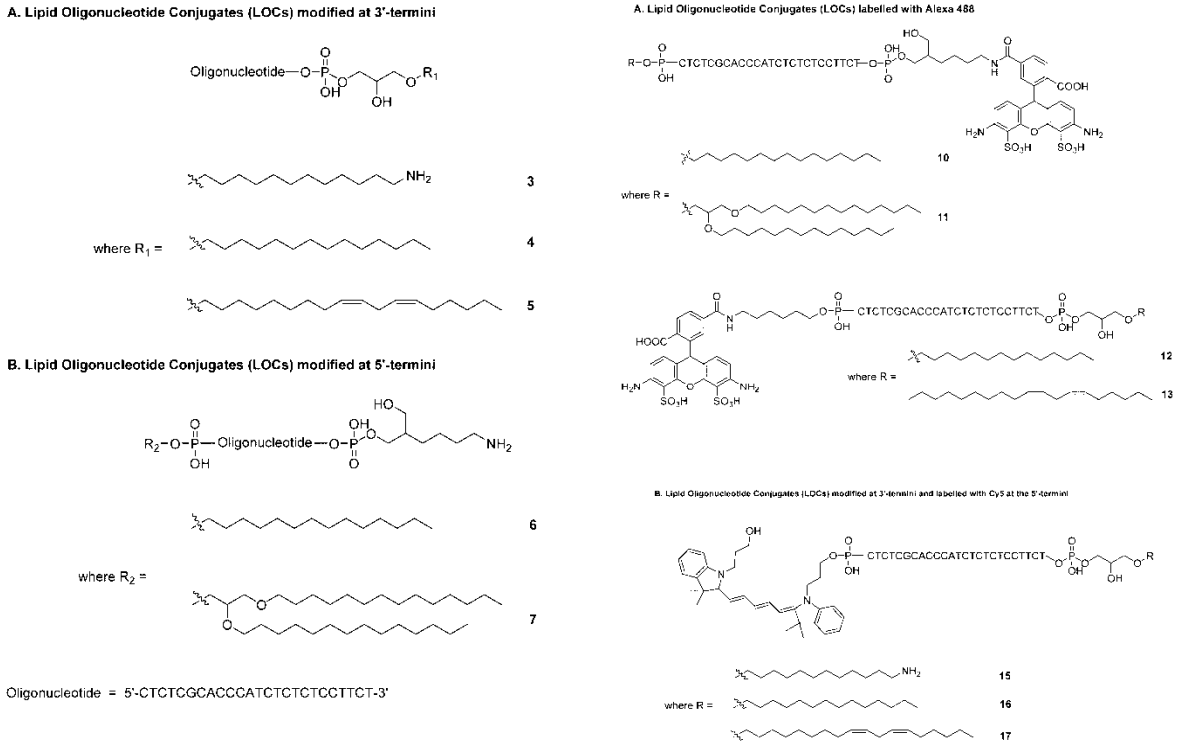

Fig. 1. Left: Schematic representation of lipid modifications introduced into the oligonucleotides**.** A) Selected lipids (R_1) were bound to the 3'-end. B) Selected lipids (R_2) were bound to the 5'-termini. Right: Schematic representation of the lipid oligonucleotide conjugates labelled with A) Alexa Fluor 488 and B) Cy5 fluorescent dyes.

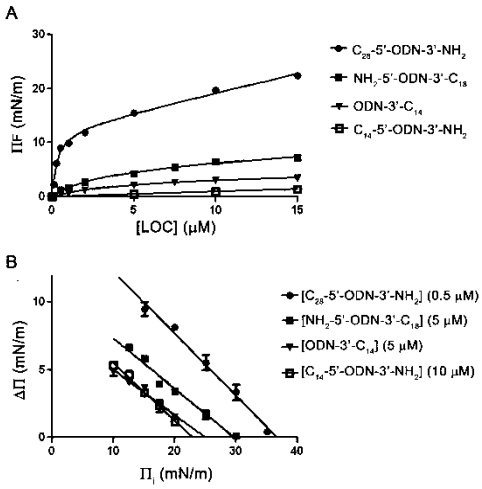

Fig. 2. Surface activity of LOCs in free-lipid and DOPC monolayes. A) Changes in surface pressure at the air-water interface induced by LOCs [compounds **4** (ODN-3'-C_{14}), **6** (C_{14}-5'-ODN-3'-NH_2), **7** (C_{28}-5'-ODN-3'-NH_2), and **9** (NH_2-5'-ODN-3'-C_{18})]. Final π values obtained from LOCs at 4,000 s incubation with constant stirring. B) Changes in surface pressure of DOPC monolayers oriented at the air-water interface as a result of LOC insertion (compounds **4**, **6**, **7** and **9**) at varying initial pressures. The plateau values of surface pressure increases ($\Delta\pi$) after LOC insertion are plotted as a function of the initial π (π_i). Average values $\pm$ SD (n=2). Subphase was 1$\times$ PBS. LOCs were injected into the subphase with constant stirring.

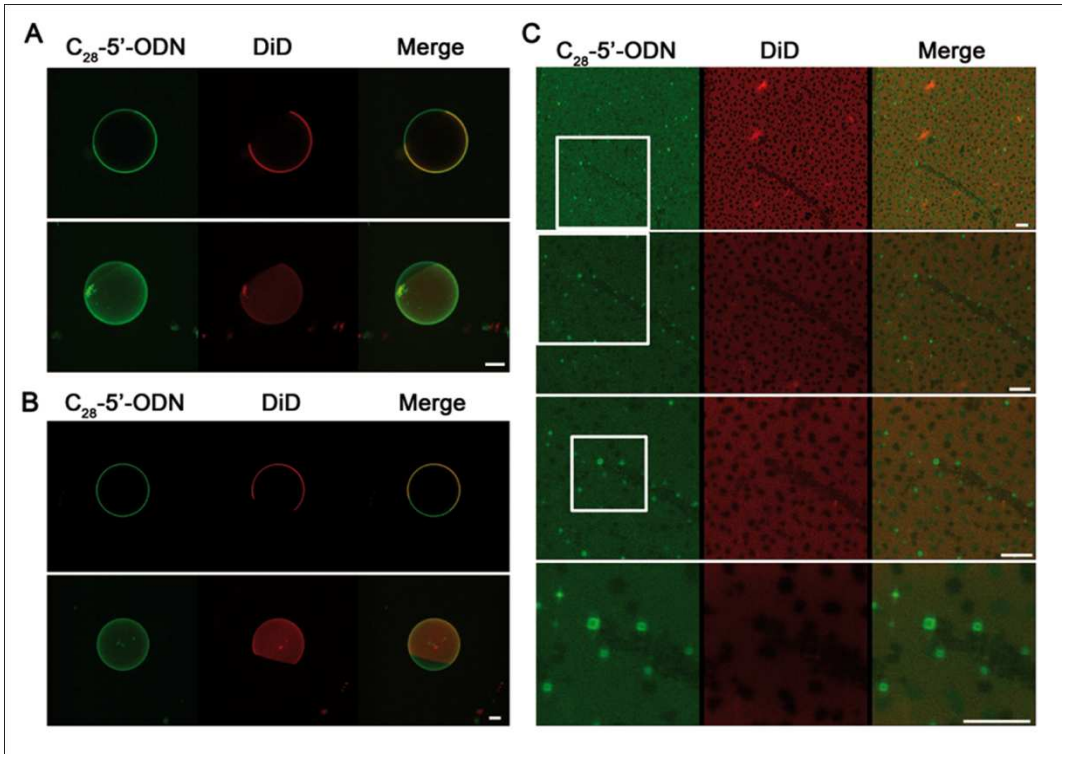

Fig. 3. Imaging of Alexa 488-labelled C_{28}-5'-ODN binding to GUVs and SPBs. Confocal microscopy images of DiD-labelled DOPC/eSM/Chol (2:2:1) GUVs [equatorial sections (upper panels); 3D reconstruction (bottom panels)] incubated with 50 nM of Alexa 488-labelled C_{28}-5'-ODN (compound **11**) for 1 h (A) and 2 h (B). Scale bars represent 5 µm. C) Confocal microscopy images of DiD-labelled DOPC/eSM/Chol (2:2:1) SPBs incubated with Alexa 488-labelled C_{28}-5'-ODN (compound **11**). First, 25 nM Alexa 488-labelled C_{28}-5'-ODN (compound **11**) were added to the SPBs and incubated for 15 min. Then, additional 25 nM Alexa 488-labelled C_{28}-5'-ODN (compound **11**) were added to the sample and incubated for another 15 min. White squares represent the zoomed regions, corresponding to the images below. LOC (green) and lipid (red) staining are shown in the left and centre columns, respectively. The right-hand side column displays the merging of both detection channels. Scale bars represent 10 µm.

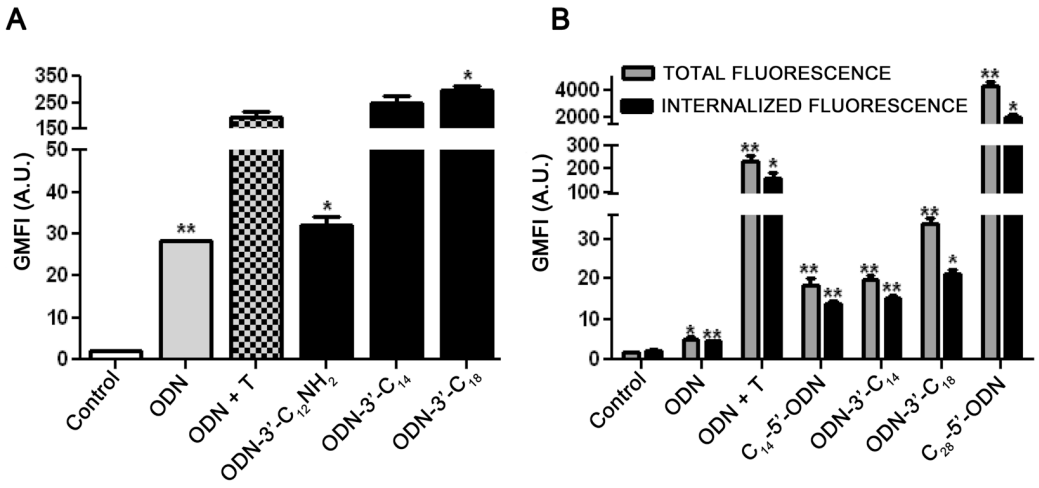

Fig. 4. Cellular binding/uptake of LOCs in HeLa cells. Cells were incubated with 500 nM Cy5- or Alexa 488-labelled control-ODNs, ODN-lipoplexes and LOCs for 4 h at 37ºC in OptiMEM. After incubation, cells were washed three times, resuspended in ice-cold PBS, and analyzed by flow cytometry. GMFI corresponds to Geometric Mean of Fluorescence Intensity. Control stands for untreated cells, representing cell basal fluorescence intensity; (ODN + T) corresponds to lipoplexes formed by the complexation of Cy5-5'-ODN (compound **18**) or ODN-3'-Alexa 488 (compound **14**) with Transfectin. Results are expressed as GMFI ± SEM of 3 independent experiments performed in duplicate (*$p<0.05$; **$p<0.01$). A) Total cellular fluorescence observed after incubation with Cy5-labelled ODN (compound **18**) and Cy5-labelled LOCs: ODN-3'-C_{12}-NH_2 (compound **15**), ODN-3'-C_{14} (compound **16**) and ODN-3'-C_{18} (compound **17**). B) Total cellular fluorescence (black columns) and internalized fluorescence (gray columns) of Alexa 488-labelled ODN (compound **14**) and Alexa 488-labelled LOCs: C_{14}-5'-ODN (compound **10**), ODN-3'-C_{14} (compound **12**), ODN-3'-C_{18} (compound **13**) and C_{28}-5'-ODN (compound **11**). Trypan Blue (0.2%, final concentration) was used to quench extracellular fluorescence.

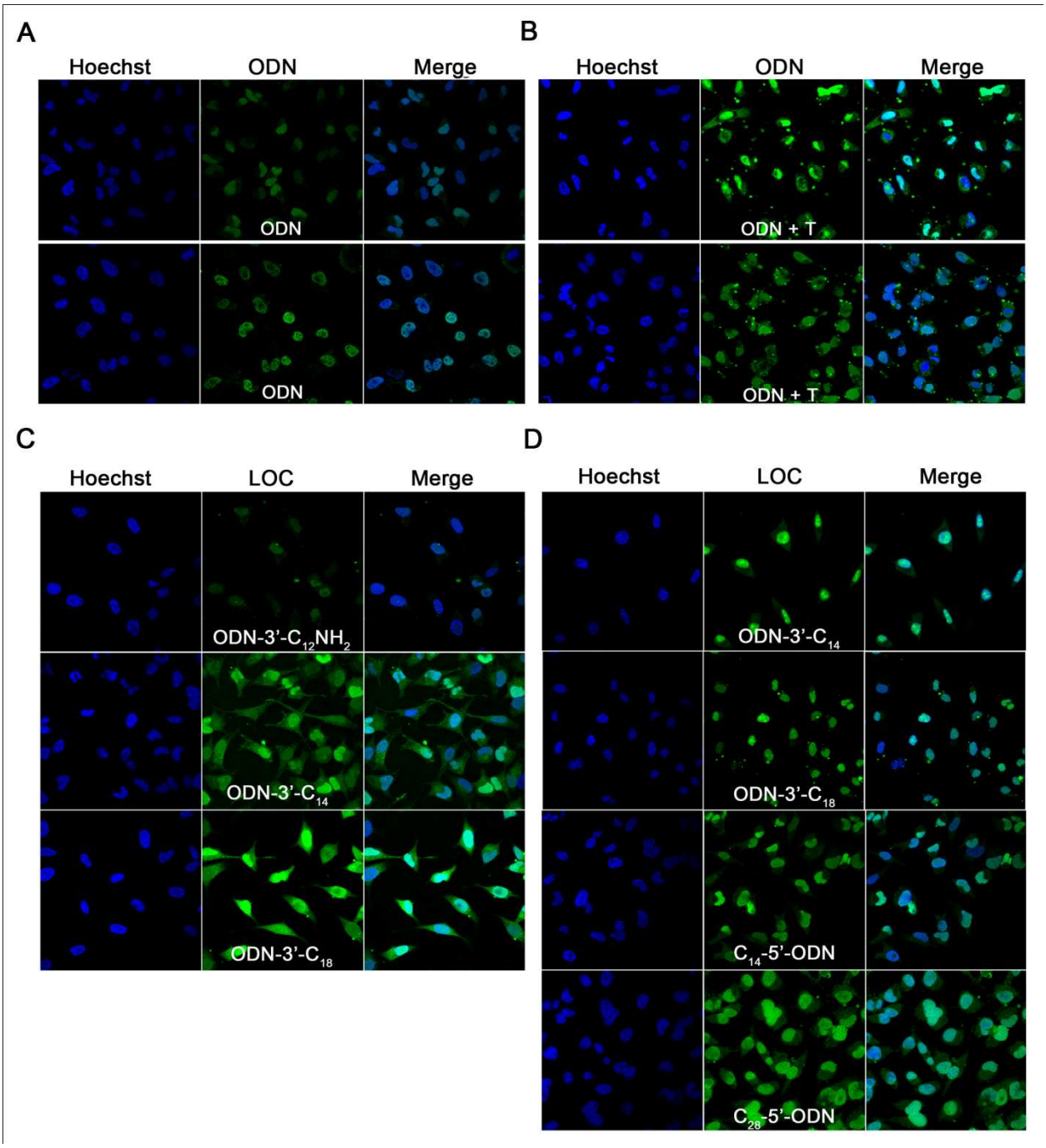

Fig. 5. Cellular uptake and subcellular localization of Cy5- and Alexa 488-labelled ODN and LOCs in HeLa cells**.** A) Cells were incubated with 500 nM Cy5-5'-ODN (compound **18**) (upper panels) or ODN-3'-Alexa 488 (compound **14**) (bottom panels) for 4h at 37ºC in OptiMEM. B) Cells were incubated with 500 nM ODN-lipoplexes for 4 h at 37ºC in OptiMEM. (ODN + T) correspond to lipoplexes formed by the complexation of Cy5-5'-ODN (compound **18**) (upper panels) or ODN-3'-Alexa 488 (compound **14**) (bottom panels) with Transfectin, respectively. C and D) Cells were incubated with 500 nM Cy5-labelled LOCs: ODN-3'-C_{12}-NH_2 (compound **15**), ODN-3'-C_{14} (compound **16**), ODN-3'-C_{18} (compound **17**) (C) and with

Alexa 488-labelled LOCs: C_{14}-5'-ODN (compound **10**), ODN-3'-C_{14} (compound **12**), ODN-3'-C_{18} (compound **13**), C_{28}-5'-ODN (compound **11**) (D) for 4 h at 37ºC in OptiMEM. After incubation, cells were washed three times, fixed with 4% (w/v) PFA and treated with Hoechst 33258 for nucleus staining. Nucleus (blue) and LOC (green) staining are shown in the left-hand and centre columns, respectively. The right-hand column displays the merging of both detection channels.

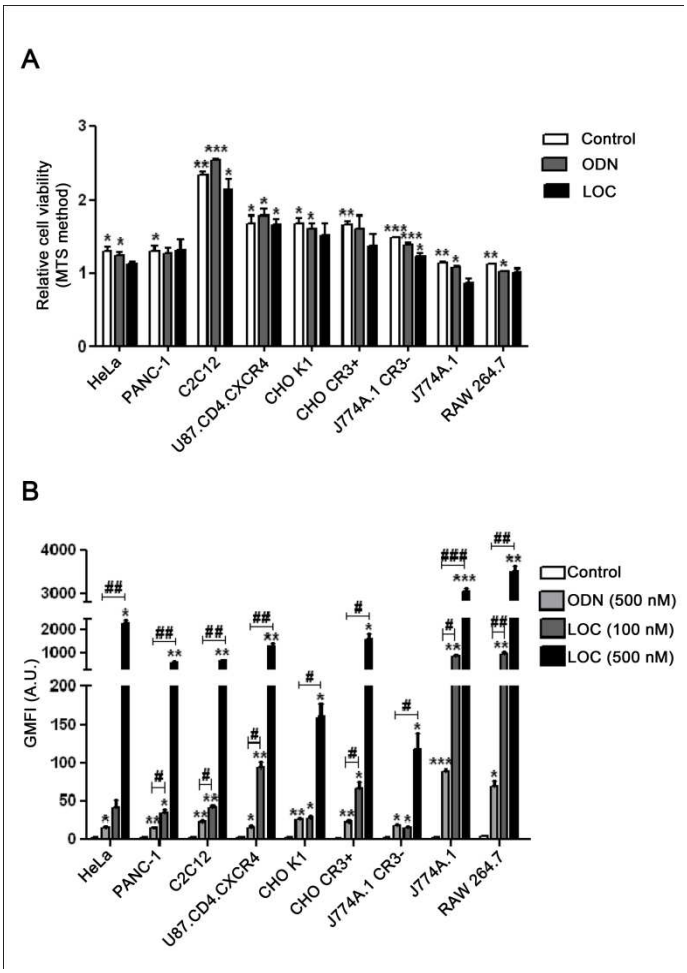

Fig. 6. Cell cytotoxicity and cellular uptake assays of C_{28}-5'-ODN in different cell lines. A) Cell cytotoxicity assay. Cells were seeded (5×10^3 cells/well) in 96 well plates and incubated overnight in appropriate growth medium. Then, cells were incubated in 100 µl OptiMEM in the absence or presence of 1 µM control-ODN (ODN) (compound **2**) or C_{28}-5'-ODN (LOC) (compound **7**) for 24 h at 37ºC. Untreated cells were used as negative control (Control). Data were normalized to the control value (untreated cells at 0 h of incubation) and are expressed as the mean ± SEM of 3 independent experiments performed in triplicate (*p<0.05; **p<0.01; *** p<0.001). B) Cellular uptake assay. Cells were seeded (1.25×10^5 cells/well) in 24 well plates and cultured overnight in appropriate growth medium. Then, cells were incubated with 500 nM ODN-3'-Alexa 488 (ODN) (compound **14**) or 100 and 500 nM Alexa 488-labelled C_{28}-5'-ODN (LOC) (compound **11**) for 4 h at 37ºC in OptiMEM. After incubation, cells were washed three times, resuspended in ice-cold PBS, and analyzed by flow cytometry. Control stands for untreated cells, representing cell basal fluorescence intensity. GMFI corresponds to Geometric Mean of Fluorescence Intensity. Results are expressed as GMFI ± SEM of 3 independent experiments performed in duplicate (*p<0.05, **p<0.01 and *** p<0.001 *vs* the control value; #p<0.05, ##p<0.01 and ###p<0.001 *vs* ODN value).

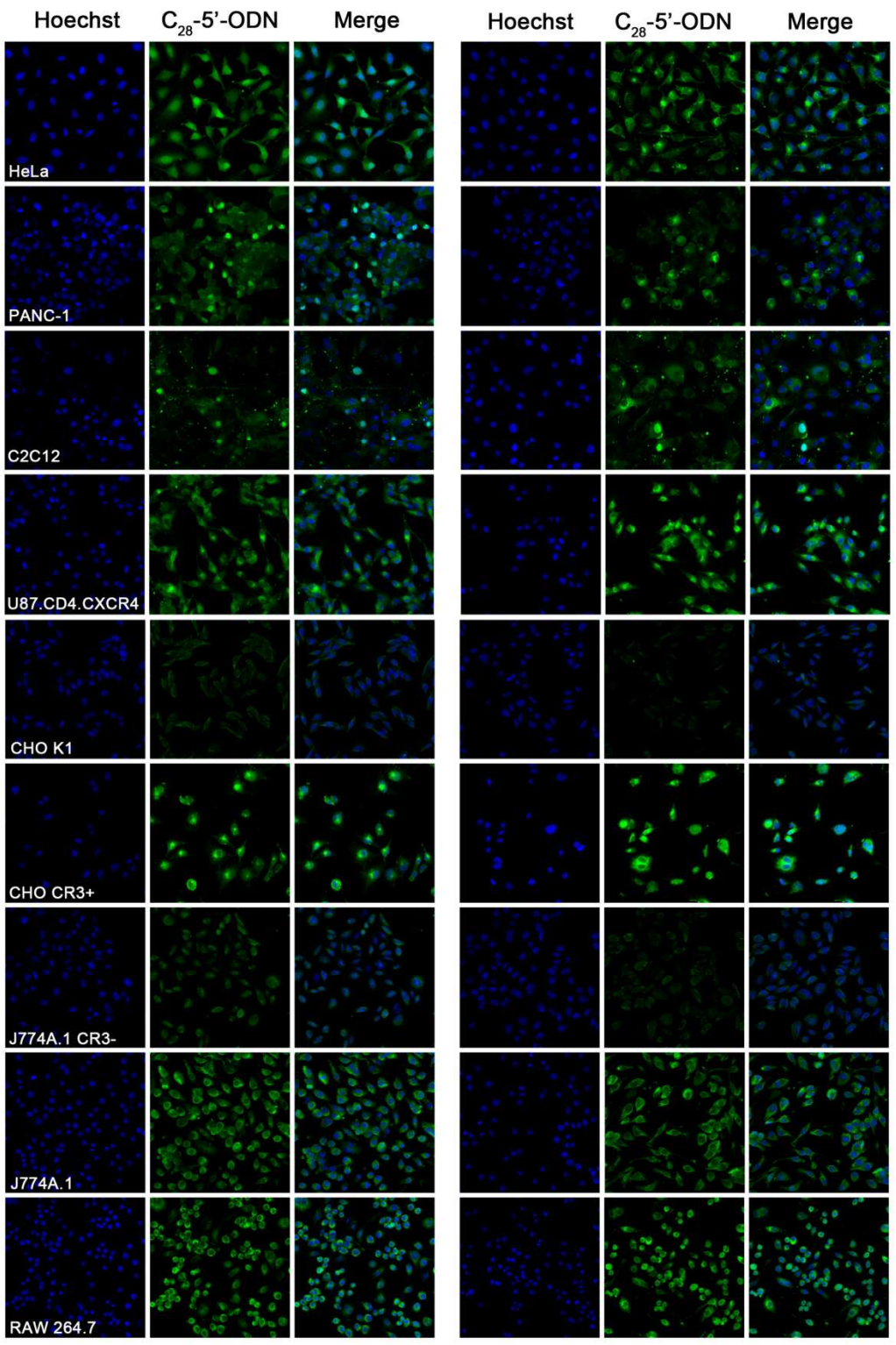

Fig. 7. Cellular uptake and subcellular localization of Alexa 488-labelled C_{28}-5'-ODN in different cell lines. Cells were incubated with 100 nM Alexa Alexa 488-labelled C_{28}-5'-ODN (compound **11**) in for 30 min (left

panels) or 4 h (right panels) at 37ºC in OptiMEM. After incubation, cells were washed three times, fixed with 4% (w/v) PFA and treated with Hoechst for nucleus staining. Nucleus (blue) and C_{28} moiety bearing LOC (green) staining are shown in the left and centre columns, respectively. The right column displays the merging of both detection channels.

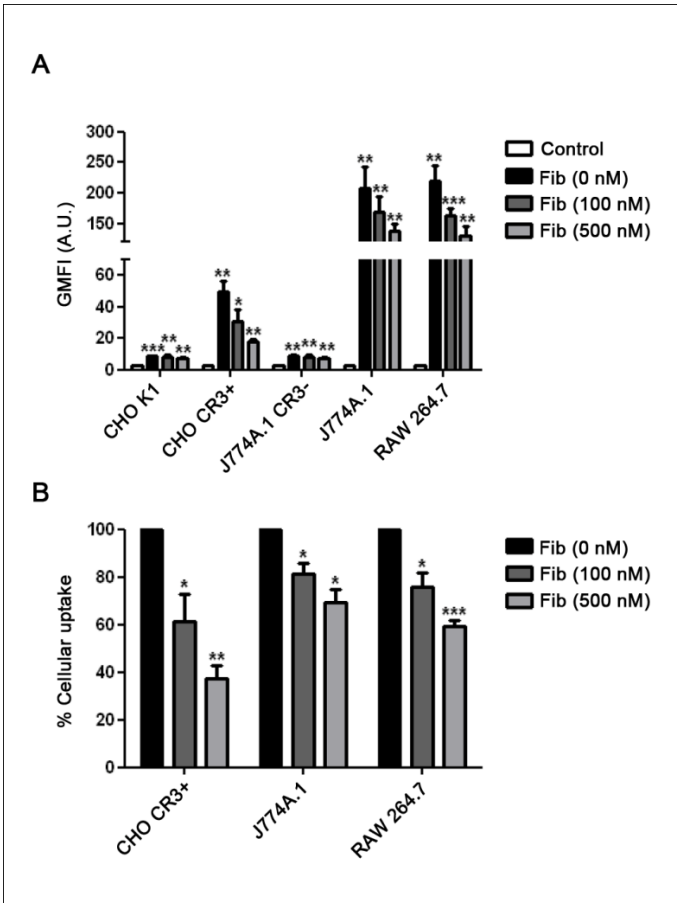

Fig. 8. Effects of the soluble fibrinogen on cellular uptake of Alexa 488-labelled C_{28}-5'-ODN in CHO K1, CHO CR3+, J774A.1 CR3-, J774A.1 and RAW264.7 cells. Cells were seeded (1.25×10^5 cells/well) in 24 well plates and cultured overnight in appropriate growth medium. Then, cells were pretreated in the presence of 100 nM or 500 nM soluble fibrinogen (Fib) for 30 min at 37ºC in OptiMEM. Next, cells were incubated with 100 nM Alexa 488-labelled C_{28}(5')-GEM91 for 30 min at 37ºC. After incubation, cells were washed three times, resuspended in ice-cold PBS, and analyzed by flow cytometry. A) LOC internalization in the presence of fibrinogen. Control stands for untreated cells, representing cell basal fluorescence intensity. GMFI corresponds to Geometric Mean of Fluorescence Intensity. Results are expressed as GMFI ± SEM of 4 independent experiments performed in duplicate (*p<0.05; **p<0.01; ***p<0.001). B) LOC internalization percentage in the presence of fibrinogen. Cellular uptake achieved in the absence of soluble fibrinogen was considered as the maximum internalization (100%). Results are expressed as percentage of cellular uptake ± SEM of 4 independent experiments performed in duplicate (*p<0.05; **p<0.01; ***p<0.001).

Tables

Table 1

MALDI-TOF spectrometry data of the oligonucleotides prepared in this study.

Compound	MW (calcd)	MW (found)
1, 5′-CTCTCGCACCCATCTCTCTCCTTCT-3′	7387	7384
2, 5′-CTCTCGCACCCATCTCTCTCCTTCT-3′-NH_2	7601	7604
3, 5’-CTCTCGCACCCATCTCTCTCCTTCT-3’-[$C_{12}NH_2$]	7725	7722
4, 5’-CTCTCGCACCCATCTCTCTCCTTCT-3’-[C_{14}]	7738	7734
5, 5’-CTCTCGCACCCATCTCTCTCCTTCT-3’-[C_{18}]	7790	7795
6, [C_{14}]-5’-CTCTCGCACCCATCTCTCTCCTTCT-3’-NH_2	7877	7882
7, [C_{28}]-5′-CTCTCGCACCCATCTCTCTCCTTCT-3′-NH_2	8147	8149
8, NH_2-5’-CTCTCGCACCCATCTCTCTCCTTCT-3’-[C_{14}]	7917	7986[1]
9, NH_2-5’-CTCTCGCACCCATCTCTCTCCTTCT-3’-[C_{18}]	7969	7962
10, [C_{14}]-5’-CTCTCGCACCCATCTCTCTCCTTCT-3’-NHCO-Alexa 488	8359	8353
11, [C_{28}]-5′-CTCTCGCACCCATCTCTCTCCTTCT-3′-NHCO-Alexa 488	8629	8631
12, Alexa 488-CONH-5’-CTCTCGCACCCATCTCTCTCCTTCT-3’-[C_{14}]	8435	8497[1,4]
13, Alexa 488-CONH-5’-CTCTCGCACCCATCTCTCTCCTTCT-3’-[C_{18}]	8472	8477[4]
14, 5’-CTCTCGCACCCATCTCTCTCCTTCT-3’-NHCO-Alexa 488	8118	8117[3]
15, Cy5-5’-CTCTCGCACCCATCTCTCTCCTTCT-3’-[C_{12} NH_2]	8273	8293[2]
16, Cy5-5’-CTCTCGCACCCATCTCTCTCCTTCT-3’-[C_{14}]	8260	8267
17, Cy5-5′-CTCTCGCACCCATCTCTCTCCTTCT-3′-[C_{18}]	8330	8328
18, Cy5-5′-CTCTCGCACCCATCTCTCTCCTTCT-3′	7920	7925

[1] [M^++Na^++K^+]

[2] [M^++Na^+]

[3] Reference [33]

[4] mixture of labelled and unlabelled oligonucleotide

Acknowledgements

This work was supported with funds from the Spanish Ministry of Economy [Grant BFU2007-62062], the Basque Government [GIV06-42], the Spanish Ministry of Education [Grant CTQ2010-20541], the Generalitat de Catalunya [2009/SGR/208], the Instituto de Salud Carlos III [CB06_01_0019] and Fundación Biofísica Bizkaia. CIBER-BBN is an iniciative funded by the VI National R&D&I Plan 2008-2011, Iniciativa Ingenio 2010, Consolider Program, CIBER Actions and financed by the Instituto de Salud Carlos III with assistance from the European Regional Development. B.U-U. was supported by Universidad de País Vasco-UPV/EHU pre-doctoral fellowship and Fundación Biofísica Bizkaia. J.V.B. was a postdoctoral scientist supported by Universidad de País Vasco-UPV/EHU postdoctoral fellowship. The authors acknowledge the Servicio General de Microscopía Analítica y de Alta Resolución en Biomedicina at the University of Basque Country for assistance with confocal microscopy, Prof. A. Gómez-Muñoz for flow cytometry facilities and Eneritz Bilbao for excellent technical assistance.

References

[1] J. Goodchild, Therapeutic oligonucleotides, Methods Mol Biol, 764 (2011) 1-15.
[2] F. Takeshita, T. Ochiya, Therapeutic potential of RNA interference against cancer, Cancer science, 97 (2006) 689-696.
[3] K.A. Whitehead, R. Langer, D.G. Anderson, Knocking down barriers: advances in siRNA delivery, Nature reviews. Drug discovery, 8 (2009) 129-138.
[4] M.A. Mintzer, E.E. Simanek, Nonviral vectors for gene delivery, Chemical reviews, 109 (2009) 259-302.
[5] M. Manoharan, Oligonucleotide conjugates as potential antisense drugs with improved uptake, biodistribution, targeted delivery, and mechanism of action, Antisense & nucleic acid drug development, 12 (2002) 103-128.
[6] H. Lonnberg, Solid-phase synthesis of oligonucleotide conjugates useful for delivery and targeting of potential nucleic acid therapeutics, Bioconjugate chemistry, 20 (2009) 1065-1094.
[7] M. Raouane, D. Desmaele, G. Urbinati, L. Massaad-Massade, P. Couvreur, Lipid Conjugated Oligonucleotides: A Useful Strategy for Delivery, Bioconjugate chemistry, (2012).
[8] Y. Singh, P. Murat, E. Defrancq, Recent developments in oligonucleotide conjugation, Chem Soc Rev, 39 (2010) 2054-2070.
[9] Y.H. Chan, B. van Lengerich, S.G. Boxer, Effects of linker sequences on vesicle fusion mediated by lipid-anchored DNA oligonucleotides, Proc Natl Acad Sci U S A, 106 (2009) 979-984.
[10] S.T. Crooke, M.J. Graham, J.E. Zuckerman, D. Brooks, B.S. Conklin, L.L. Cummins, M.J. Greig, C.J. Guinosso, D. Kornbrust, M. Manoharan, H.M. Sasmor, T. Schleich, K.L. Tivel, R.H. Griffey, Pharmacokinetic properties of several novel oligonucleotide analogs in mice, The Journal of pharmacology and experimental therapeutics, 277 (1996) 923-937.
[11] B.S. Herbert, G.C. Gellert, A. Hochreiter, K. Pongracz, W.E. Wright, D. Zielinska, A.C. Chin, C.B. Harley, J.W. Shay, S.M. Gryaznov, Lipid modification of GRN163, an N3'-->P5' thio-phosphoramidate oligonucleotide, enhances the potency of telomerase inhibition, Oncogene, 24 (2005) 5262-5268.
[12] C. MacKellar, D. Graham, D.W. Will, S. Burgess, T. Brown, Synthesis and physical properties of anti-HIV antisense oligonucleotides bearing terminal lipophilic groups, Nucleic acids research, 20 (1992) 3411-3417.
[13] M. Manoharan, in: R.M. Crooke (Ed.) Antisense Drug Technology, Marcel Dekker Inc., New York, 2001, pp. 391-469.
[14] K. Nishina, T. Unno, Y. Uno, T. Kubodera, T. Kanouchi, H. Mizusawa, T. Yokota, Efficient in vivo delivery of siRNA to the liver by conjugation of alpha-tocopherol, Molecular therapy : the journal of the American Society of Gene Therapy, 16 (2008) 734-740.
[15] A.S. Boutorin, L.V. Gus'kova, E.M. Ivanova, N.D. Kobetz, V.F. Zarytova, A.S. Ryte, L.V. Yurchenko, V.V. Vlassov, Synthesis of alkylating oligonucleotide derivatives containing cholesterol or phenazinium residues at their 3'-terminus and their interaction with DNA within mammalian cells, FEBS letters, 254 (1989) 129-132.
[16] D. De Paula, M.V. Bentley, R.I. Mahato, Hydrophobization and bioconjugation for enhanced siRNA delivery and targeting, RNA, 13 (2007) 431-456.
[17] J.H. Jeong, H. Mok, Y.K. Oh, T.G. Park, siRNA conjugate delivery systems, Bioconjugate chemistry, 20 (2009) 5-14.
[18] C. Lorenz, P. Hadwiger, M. John, H.P. Vornlocher, C. Unverzagt, Steroid and lipid conjugates of siRNAs to enhance cellular uptake and gene silencing in liver cells, Bioorganic & medicinal chemistry letters, 14 (2004) 4975-4977.
[19] R.G. Shea, J.C. Marsters, N. Bischofberger, Synthesis, hybridization properties and antiviral activity of lipid-oligodeoxynucleotide conjugates, Nucleic acids research, 18 (1990) 3777-3783.
[20] S. Grijalvo, S.M. Ocampo, J.C. Perales, R. Eritja, Synthesis of oligonucleotides carrying amino lipid groups at the 3'-end for RNA interference studies, The Journal of organic chemistry, 75 (2010) 6806-6813.
[21] S. Grijalvo, S.M. Ocampo, J.C. Perales, R. Eritja, Synthesis of lipid-oligonucleotide conjugates for RNA interference studies, Chemistry & biodiversity, 8 (2011) 287-299.
[22] J. Sot, M. Ibarguren, J.V. Busto, L.R. Montes, F.M. Goni, A. Alonso, Cholesterol displacement by ceramide in sphingomyelin-containing liquid-ordered domains, and generation of gel regions in giant lipidic vesicles, FEBS letters, 582 (2008) 3230-3236.

[23] J. Jass, T. Tjarnhage, G. Puu, From liposomes to supported, planar bilayer structures on hydrophilic and hydrophobic surfaces: an atomic force microscopy study, Biophysical journal, 79 (2000) 3153-3163.
[24] P. Gangoiti, M.H. Granado, S.W. Wang, J.Y. Kong, U.P. Steinbrecher, A. Gomez-Munoz, Ceramide 1-phosphate stimulates macrophage proliferation through activation of the PI3-kinase/PKB, JNK and ERK1/2 pathways, Cellular signalling, 20 (2008) 726-736.
[25] R.S. Hundal, B.S. Salh, J.W. Schrader, A. Gomez-Munoz, V. Duronio, U.P. Steinbrecher, Oxidized low density lipoprotein inhibits macrophage apoptosis through activation of the PI 3-kinase/PKB pathway, Journal of lipid research, 42 (2001) 1483-1491.
[26] A. Bene, R.C. Kurten, T.C. Chambers, Subcellular localization as a limiting factor for utilization of decoy oligonucleotides, Nucleic acids research, 32 (2004) e142.
[27] X. Ming, M.R. Alam, M. Fisher, Y. Yan, X. Chen, R.L. Juliano, Intracellular delivery of an antisense oligonucleotide via endocytosis of a G protein-coupled receptor, Nucleic acids research, 38 (2010) 6567-6576.
[28] T. Ohrt, D. Merkle, K. Birkenfeld, C.J. Echeverri, P. Schwille, In situ fluorescence analysis demonstrates active siRNA exclusion from the nucleus by Exportin 5, Nucleic acids research, 34 (2006) 1369-1380.
[29] N.S. Petrova, I.V. Chernikov, M.I. Meschaninova, I.S. Dovydenko, A.G. Venyaminova, M.A. Zenkova, V.V. Vlassov, E.L. Chernolovskaya, Carrier-free cellular uptake and the gene-silencing activity of the lipophilic siRNAs is strongly affected by the length of the linker between siRNA and lipophilic group, Nucleic acids research, 40 (2012) 2330-2344.
[30] A.G. Torres, M.M. Fabani, E. Vigorito, D. Williams, N. Al-Obaidi, F. Wojciechowski, R.H. Hudson, O. Seitz, M.J. Gait, Chemical structure requirements and cellular targeting of microRNA-122 by peptide nucleic acids anti-miRs, Nucleic acids research, 40 (2012) 2152-2167.
[31] J. Lisziewicz, D. Sun, F.F. Weichold, A.R. Thierry, P. Lusso, J. Tang, R.C. Gallo, S. Agrawal, Antisense oligodeoxynucleotide phosphorothioate complementary to Gag mRNA blocks replication of human immunodeficiency virus type 1 in human peripheral blood cells, Proc Natl Acad Sci U S A, 91 (1994) 7942-7946.
[32] N.H. Nam, S. Sardari, M. Selecky, K. Parang, Carboxylic acid and phosphate ester derivatives of fluconazole: synthesis and antifungal activities, Bioorganic & medicinal chemistry, 12 (2004) 6255-6269.
[33] B. Ugarte-Uribe, S. Perez-Rentero, R. Lucas, A. Avino, J.J. Reina, I. Alkorta, R. Eritja, J.C. Morales, Synthesis, cell-surface binding, and cellular uptake of fluorescently labeled glucose-DNA conjugates with different carbohydrate presentation, Bioconjugate chemistry, 21 (2010) 1280-1287.
[34] L. Caseli, C.P. Pascholati, F. Teixeira, Jr., S. Nosov, C. Vebert, A.H. Mueller, O.N. Oliveira, Jr., Interaction of oligonucleotide-based amphiphilic block copolymers with cell membrane models, Journal of colloid and interface science, 347 (2010) 56-61.
[35] E.A. Montanha, F.J. Pavinatto, L. Caseli, O. Kaczmarek, J. Liebscher, D. Huster, O.N. Oliveira, Jr., Properties of lipophilic nucleoside monolayers at the air-water interface, Colloids and surfaces. B, Biointerfaces, 77 (2010) 161-165.
[36] J.V. Busto, J. Sot, F.M. Goni, F. Mollinedo, A. Alonso, Surface-active properties of the antitumour ether lipid 1-O-octadecyl-2-O-methyl-rac-glycero-3-phosphocholine (edelfosine), Biochim Biophys Acta, 1768 (2007) 1855-1860.
[37] D. Marsh, Lateral pressure in membranes, Biochim Biophys Acta, 1286 (1996) 183-223.
[38] B. Apellaniz, A.J. Garcia-Saez, N. Huarte, R. Kunert, K. Vorauer-Uhl, H. Katinger, P. Schwille, J.L. Nieva, Confocal microscopy of giant vesicles supports the absence of HIV-1 neutralizing 2F5 antibody reactivity to plasma membrane phospholipids, FEBS letters, 584 (2010) 1591-1596.
[39] T.J. McIntosh, S.A. Simon, Bilayers as protein solvents: role of bilayer structure and elastic properties, The Journal of general physiology, 130 (2007) 225-227.
[40] G. van Meer, Cellular lipidomics, EMBO J, 24 (2005) 3159-3165.
[41] P.K. Maiti, T. Çagin, S. Lin, W.A. Goddard, Effect of Solvent and pH on the Structure of PAMAM Dendrimers, Macromolecules, 38 (2005) 979-991.
[42] R.C. van Duijvenbode, M. Borkovec, G.J.M. Koper, Acid-base Properties of Poly(propylene imine) Dendrimers, Polymers, 39 (1998) 2657-2664.
[43] S.P. Gordon, S. Berezhna, D. Scherfeld, N. Kahya, P. Schwille, Characterization of interaction between cationic lipid-oligonucleotide complexes and cellular membrane lipids using confocal imaging and fluorescence correlation spectroscopy, Biophysical journal, 88 (2005) 305-316.

[44] V.M. Meidan, J.S. Cohen, N. Amariglio, D. Hirsch-Lerner, Y. Barenholz, Interaction of oligonucleotides with cationic lipids: the relationship between electrostatics, hydration and state of aggregation, Biochim Biophys Acta, 1464 (2000) 251-261.
[45] S. Weisman, D. Hirsch-Lerner, Y. Barenholz, Y. Talmon, Nanostructure of cationic lipid-oligonucleotide complexes, Biophysical journal, 87 (2004) 609-614.
[46] D.A. Zacharias, J.D. Violin, A.C. Newton, R.Y. Tsien, Partitioning of lipid-modified monomeric GFPs into membrane microdomains of live cells, Science, 296 (2002) 913-916.
[47] P.A. Beales, T.K. Vanderlick, Partitioning of membrane-anchored DNA between coexisting lipid phases, The journal of physical chemistry. B, 113 (2009) 13678-13686.
[48] A. Bunge, M. Loew, P. Pescador, A. Arbuzova, N. Brodersen, J. Kang, L. Dahne, J. Liebscher, A. Herrmann, G. Stengel, D. Huster, Lipid membranes carrying lipophilic cholesterol-based oligonucleotides--characterization and application on layer-by-layer coated particles, The journal of physical chemistry. B, 113 (2009) 16425-16434.
[49] J.M. Boggs, Intermolecular hydrogen bonding between lipids: influence on organization and function of lipids in membranes, Canadian journal of biochemistry, 58 (1980) 755-770.
[50] H. Taguchi, W.L. Armarego, Glyceryl-ether monooxygenase [EC 1.14.16.5]. A microsomal enzyme of ether lipid metabolism, Medicinal research reviews, 18 (1998) 43-89.
[51] C. Gosse, A. Boutorine, I. Aujard, M. Chami, A. Kononov, E. Cogne-Laage, J.F. Allemand, J. Li, L. Jullien, Micelles of Lipid-Oligonucleotide Conjugates: Implications for Membrane Anchoring and Base Pairing, The journal of physical chemistry. B, 108 (2004) 6485-6497.
[52] B.D. Chithrani, A.A. Ghazani, W.C. Chan, Determining the size and shape dependence of gold nanoparticle uptake into mammalian cells, Nano letters, 6 (2006) 662-668.
[53] J. Dausend, A. Musyanovych, M. Dass, P. Walther, H. Schrezenmeier, K. Landfester, V. Mailander, Uptake mechanism of oppositely charged fluorescent nanoparticles in HeLa cells, Macromolecular bioscience, 8 (2008) 1135-1143.
[54] T. dos Santos, J. Varela, I. Lynch, A. Salvati, K.A. Dawson, Effects of transport inhibitors on the cellular uptake of carboxylated polystyrene nanoparticles in different cell lines, PloS one, 6 (2011) e24438.
[55] F. Osaki, T. Kanamori, S. Sando, T. Sera, Y. Aoyama, A quantum dot conjugated sugar ball and its cellular uptake. On the size effects of endocytosis in the subviral region, Journal of the American Chemical Society, 126 (2004) 6520-6521.
[56] R. Leventis, J.R. Silvius, Interactions of mammalian cells with lipid dispersions containing novel metabolizable cationic amphiphiles, Biochim Biophys Acta, 1023 (1990) 124-132.
[57] L.H. Lindner, R. Brock, D. Arndt-Jovin, H. Eibl, Structural variation of cationic lipids: minimum requirement for improved oligonucleotide delivery into cells, Journal of controlled release : official journal of the Controlled Release Society, 110 (2006) 444-456.
[58] K.T. Love, K.P. Mahon, C.G. Levins, K.A. Whitehead, W. Querbes, J.R. Dorkin, J. Qin, W. Cantley, L.L. Qin, T. Racie, M. Frank-Kamenetsky, K.N. Yip, R. Alvarez, D.W. Sah, A. de Fougerolles, K. Fitzgerald, V. Koteliansky, A. Akinc, R. Langer, D.G. Anderson, Lipid-like materials for low-dose, in vivo gene silencing, Proc Natl Acad Sci U S A, 107 (2010) 1864-1869.
[59] L. Xu, T. Anchordoquy, Drug delivery trends in clinical trials and translational medicine: challenges and opportunities in the delivery of nucleic acid-based therapeutics, Journal of pharmaceutical sciences, 100 (2011) 38-52.
[60] T. Kubo, K. Yanagihara, Y. Takei, K. Mihara, Y. Morita, T. Seyama, Palmitic acid-conjugated 21-nucleotide siRNA enhances gene-silencing activity, Molecular pharmaceutics, 8 (2011) 2193-2203.
[61] S.J. Forsha, I.V. Panyutin, R.D. Neumann, I.G. Panyutin, Intracellular traffic of oligodeoxynucleotides in and out of the nucleus: effect of exportins and DNA structure, Oligonucleotides, 20 (2010) 277-284.
[62] L. Benimetskaya, J.D. Loike, Z. Khaled, G. Loike, S.C. Silverstein, L. Cao, J. el Khoury, T.Q. Cai, C.A. Stein, Mac-1 (CD11b/CD18) is an oligodeoxynucleotide-binding protein, Nature medicine, 3 (1997) 414-420.
[63] P. Watson, A.T. Jones, D.J. Stephens, Intracellular trafficking pathways and drug delivery: fluorescence imaging of living and fixed cells, Advanced drug delivery reviews, 57 (2005) 43-61.
[64] R. Kirsch, M.A. Jaffer, V.E. Woodburne, T. Sewell, S.L. Kelly, R.E. Kirsch, E.G. Shephard, Fibrinogen is degraded and internalized during incubation with neutrophils, and fibrinogen products localize to electron lucent vesicles, The Biochemical journal, 364 (2002) 403-412.

[65] V.K. Lishko, N.P. Podolnikova, V.P. Yakubenko, S. Yakovlev, L. Medved, S.P. Yadav, T.P. Ugarova, Multiple binding sites in fibrinogen for integrin alphaMbeta2 (Mac-1), The Journal of biological chemistry, 279 (2004) 44897-44906.
[66] L. Zhou, D.H. Lee, J. Plescia, C.Y. Lau, D.C. Altieri, Differential ligand binding specificities of recombinant CD11b/CD18 integrin I-domain, The Journal of biological chemistry, 269 (1994) 17075-17079.